ANALYSIS OF REACTION RATE DISTRIBUTIONS ON A THICK TUNGSTEN TARGET BOMBARDED WITH PROTONS OF 0.8 TO 1.2 GEV

H. Takada, S. Meigo, T. Sasa, T. Fukahori
Japan Atomic Energy Research Institute
Tokai-mura, Naka-gun, Ibaraki-ken, JAPAN

V. I. Belyakov-Bodin, G. I. Krupny
Institute of Theoretical and Experimental Physics,
B.Cheremushkinskaya, 25, Moscow, RUSSIA

Yu. E. Titarenko
Institute of High Energy Physics,
Protvino, Moscow Region, RUSSIA

Abstract

In order to estimate the accuracy of the NMTC/JAERI-MCNP-4A code system, an analytical study is performed for the distributions of reaction rates of various activation samples on the surface of a cylindrical thick tungsten target bombarded with 0.8 and 1.2 GeV protons. It is found through the comparison between the experiment and calculation that the NMTC/JAERI-MCNP-4A code system can represent the reaction rates of the activation detectors which are sensitive to the sub-10 MeV neutrons with an accuracy of 10 to 15%. As the threshold energy of the activation detector increases, however, the agreement becomes worse. The calculated results are 50 to 75% in the C/E ratios for the activation detectors sensitive to the neutrons with tens of MeV. The disagreement suggests that the NMTC/JAERI estimates too low the production of neutrons with energies of several tens of MeV in the thick target.

1. Introduction

An accelerator-driven subcritical system is proposed as one of options for the transmutation of long-lived transuranic (TRU) nuclides. Various concepts[1-5] have been proposed for the accelerator-driven transmutation systems. Many of them adopt the design concept that the subcritical core consists of a spallation neutron target surrounded with a blanket including TRU fuels. The target is bombarded with intermediate energy protons of 0.8 to 1.6 GeV with a current of several tens of mA. A heavy metal such as tungsten and lead has been generally selected as target material in design studies because it has high neutron yield of a couple of tens of neutrons per incident proton and can suppress the power density distribution within an acceptable level.

The neutron yield and source neutron energy spectra are important factors to characterize not only the neutronic performance of the subcritical core but for the shielding design. The neutronic calculation of accelerator-based transmutation systems has been carried out with a Monte Carlo simulation code system combining the nucleon-meson transport code such as LAHET[6], HETC-KFA[7] and NMTC/JAERI[8] with the neutron transport code of MORSE[9] and MCNP[10]. Since there are few available nuclear data covering the energy region up to a few GeV yet, it is necessary to enhance the accuracy of the nucleon-meson transport code for detailed neutronic design studies.

It is known that the nucleon-meson transport codes can describe the spallation reaction qualitatively well. However, there still remains some points to be improved in the code. Those aspects were recently confirmed through a code intercomparison conducted by OECD/NEA[11-13]. In JAERI, we have also been estimating the accuracy of the NMTC/JAERI code in comparison with our own experimental data[14-18] in the intermediate energy region of 40 MeV to 3.0 GeV.

As an extension of the study, a reaction rate distribution measurement on a thick tungsten target was carried out using protons of 0.8, 1.0 and 1.2 GeV as a cooperative work between JAERI and Institute of Theoretical and Experimental Physics under the contract of International Science and Technology Center project #157. Analytical study has just started using the NMTC/JAERI-MCNP-4A code system. This paper presents the comparison of the calculated results with experimental ones for the reaction rates of some activation detectors for 0.8 and 1.2 GeV proton incidence.

2. Experimentals

The experiment was carried out at the booster beam line of Institute of High Energy Physics in Russia. In the experiment, 0.8, 1.0 and 1.2 GeV protons were injected into a cylindrical tungsten target having the size of 20 cm in diameter and 60 cm in length. The purity and density of the tungsten target was 19.1 g/cc and 99.95%, respectively. Reaction rate distributions on the cylindrical side surface of the target were measured using various kinds of activation detectors. For the 0.8 and 1.2 GeV proton incidence, the high purity foils of ^{27}Al, ^{12}C, ^{31}P, ^{32}S, ^{103}Rh, ^{115}In, ^{197}Au and ^{209}Bi were put on the side surface at the distances of 2, 8, 12, 17, 30 and 55 cm from the beam incident surface. In this study, the reaction rates of the ^{27}Al, ^{31}P, ^{32}S and ^{209}Bi samples were analyzed. The physical and nuclear characteristics of the activation detectors are summarized in Tables 1 and 2, respectively.

During the irradiation period, proton beam intensity was monitored using an induction current sensor with an accuracy of about 3 %. The profile of the beam was the Gaussian distribution with a FWHM of 2.4 cm. The number of protons injected in the target was 1.3×10^{14} to 4.3×10^{15}. The γ and β rays from the activation detectors were measured using Ge-detectors and polystyrene scintillation counters, respectively. The error in determining the activities of the activation samples were less than 3% at 0.95 confidence level for the γ-ray measurement, while less than 22% at 0.95 confidence level for the β-ray measurement.

3. Calculation

The calculation was carried out using the nucleon meson transport code NMTC/JAERI and the continuous energy Monte Carlo code MCNP-4A. The flow of the calculational procedure is shown in Fig. 1. NMTC/JAERI calculated the nuclear reactions on the basis of the intranuclear cascade[19] evaporation[20] model including the high energy fission process[21] and also simulated the particle transport in a thick medium. The parametrized in-medium nucleon-nucleon (NN) cross sections[22] similar to those of Cugnon[23] were employed instead of the free NN ones in the intranuclear cascade calculation. The level density parameter derived by Ignatyuk[24] with the parameters proposed by Mengoni et al.[25] was selected in the evaporation calculation. In

the particle transport calculation, the cutoff energy was set to be 5 MeV for charged particles and 20 MeV for neutron. The nucleon-nucleus collision cross sections based on the systematics derived by Pearlstein[26] were employed in the energy region below 1 GeV, while the geometric cross sections were used in the energy region above 1 GeV. The transport of neutrons in the energy region below 20 MeV was calculated with MCNP-4A using a continuous energy cross section library, FSXLIB-J3R2[27], which was processed from the nuclear data file JENDL-3.2[28]. Here, the neutron induced nuclear reactions below 20 MeV are taken into account as the cross section data in FSXLIB-J3R2.

Reaction rate of the activation detector, j, on the cylindrical surface of the tungsten target is obtained as

$$R_j = \int_{Eth}^{Emax} \sigma_j(E)\phi(E)dE \quad , \tag{1}$$

where $\sigma_j(E)$ represents the nuclide production cross section and $\phi(E)$ stands for the neutron or proton flux. In this calculation, the energy group structure defined in the HILO-86R library[29] was employed up to 400 MeV. In order to cover the higher energy region, supplemental energy groups of 50 MeV interval were added up to 800 MeV and then those of 100 MeV one were given between 800 and 1200 MeV.

As for the nuclide production cross section, the data of JENDL Dosimetry file[30] were used in the MCNP-4A code in the energy region below 20 MeV. In the energy region above 20 MeV, on the other hand, the nuclide production cross sections were calculated with the ALICE-F code[31] at the energy boundary of the energy group structure. The cross section in each energy group was obtained by the weighted average of the calculated values with 1/E spectrum.

The neutron or proton flux was calculated with the NMTC-JAERI-MCNP-4A code system for the incident protons of 400,000 with the revised data and parameters described above. The profile of proton beam was selected as the gaussian distribution of 2.4 cm in FWHM. In the error estimation, the statistical error of the neutrons counted in each energy group was only taken into account. The ambiguity of the nuclide production cross section was not included. For the C/E ratios, the error was obtained from the experimental error and the statistical error in the calculation based on the propagation theory.

The contribution of leakage protons to the reaction rates was estimated with the nuclide production cross sections calculated with ALICE-F. It was found that the contribution of the proton induced reactions was so small as a few percent of the total reaction rate even in the most sensitive case. In consequence, the calculated results of the neutron induced reaction are compared with the experimental ones in the following discussion.

4. Results and Discussion

The calculated reaction rates are compared with the experimental ones in Figs. 2 to 5. The C/E rations of the reactions are shown in Fig. 6. The sensitivity of the reaction rates to the neutron energy are shown in Fig. 7 for the activation detectors whose threshold energies are lower than 20 MeV. It is observed in Fig. 2 that the calculated reaction rate distributions agree well with those of experimental ones for all the reactions at incident energy of 0.8 GeV. Judging from the results of C/E ratios, good agreement is obtained between the calculated and experimental reaction rates of $^{32}S(n,p)^{32}P$ and $^{27}Al(n,p)^{27}Mg$. A large difference appears between the calculated and experimental results of the $^{31}P(n,p)^{31}Si$ reaction in the region from 2 to 12 cm. For the $^{27}Al(n,p)^{24}Na$ reaction, the calculated reaction rates are constantly lower than the experimental ones about 25 to 30% at all the positions. The most sensitive neutron energy is between 8 and 25 MeV for this reaction as seen in Fig. 7. Since the ambiguity of the cross section data of the $^{27}Al(n,p)^{24}Na$ reaction is not so large as 30% in that energy region, the disagreement indicates that the NMTC/JAERI-MCNP-4A code system estimates the leakage neutron in that energy region as low as about 25 to 30%.

As shown in Fig. 3, the agreement between the calculated and experimental reaction rates is poor for the activation detectors with higher threshold energy. It is observed in Fig. 6 that the calculated results are about 25 to 30% lower than the experimental ones for $^{209}Bi(n,4n)^{206}Bi$, $^{209}Bi(n,5n)^{205}Bi$, and $^{209}Bi(n,7n)^{203}Bi$. As far as the $^{209}Bi(n,6n)^{204}Bi$ reaction is concerned, a significant disagreement of a factor of 2 or more is observed between the calculated and experimental results. The sensitivity of the reaction rates to the neutron energy are shown in Fig. 8 for the $^{209}Bi(n,xn)$ reactions. The $^{209}Bi(n,6n)^{204}Bi$ reaction is dominant in the energy range of 45 to 90 MeV. Figures 9 to 12 compare the calculated nuclide production cross sections of the $^{209}Bi(n, xn)$ reactions with

recent experimental results[32]. It is observed that the calculated nuclide cross sections are in fairly good agreement with the experiment ones and never deviate from those more than a factor of 2 in the sensitive energy region of 45 to 90 MeV. Therefore, the disagreement in the ^{209}Bi(n, xn) reactions seems to mainly come from the underestimation of the amount of leakage neutron by the NMTC/JAERI calculation.

For the 1.2 GeV proton incidence, it is observed in Figs. 4 and 6 that the calculated results are in good agreement with the experimental ones for the ^{32}S(n,p)^{32}P reaction except at the distance of 55 cm. The fairly good agreement is obtained in the results of the ^{31}P(n,p)^{31}Si reaction although the calculated results are slightly higher than the experimental ones. The calculated reaction rates of the ^{27}Al(n,p)^{27}Mg reaction are lower than the experimental results by 15 to 20% near the front surface, while they agree well with the experimental results between 12 and 30 cm. A significant underestimation of 21 to 34% is observed in the results of the ^{27}Al(n,p)^{24}Na reaction except for the position of 55 cm. This is the same tendency as for the analysis of the 0.8 GeV proton incidence.

In Fig. 4, it should be noted that the experimental reaction rates decrease rapidly from 30 cm to 55 cm. Such phenomena, on the other hand, do not appear in the calculated results. This leads to the significantly large C/E ratios at 55 cm for those reactions although they are not shown in Fig. 6. The neutron production at the deep position seems to be estimated too large by the reason that the mean free path of high energy neutron or proton is overestimated by NMTC/JAERI. This problem is, however, not resolved for the time being.

As far as the ^{209}Bi(n,xn) reactions are concerned, the NMTC/JAERI calculation again gives lower reaction rates than the experimental ones as seen in Fig. 5. Judging from the C/E rations shown in Fig. 6, the degree of agreement is almost the same as for the case of the 0.8 GeV proton incidence. The C/E ratios of the ^{209}Bi(n,4n)^{206}Bi reaction are poorer than that for the 0.8 GeV proton incidence. These results indicate that the present NMTC/JAERI code estimates the production of neutrons with energies of several tens of MeV too low even for the 1.2 GeV proton incidence. At the position of 55 cm, the phenomena mentioned above does not appear for the ^{209}Bi(n,xn) reactions.

The present NMTC/JAERI code has already been employed in the analysis[16] of the neutron spectra of a thick lead target bombarded with the 0.5 and 1.5 GeV protons. It was pointed out in Ref. 16 that the code gave lower neutron yield than the experimental results especially in the energy region between 20 and 80 MeV. The present analysis points out the same feature of NMTC/JAERI as for the previous one. Since various microscopic factors are mixed in the results of integral experiment, the cause of the problem is not attributed only to the treatment of the nuclear reaction process. It is also necessary to investigate the accuracy of the nucleon-nucleus cross sections employed in the energy region above 20 MeV.

At last, a large fluctuation is observed in the C/E ratios of a part of the reaction rates, e.g. ^{209}Bi(n,4n)^{206}Bi and ^{209}Bi(n,7n)^{203}Bi at the distance of 30 cm for the 0.8 GeV proton incidence. Some additional error may be included in those experimental results.

5. Concluding Remarks

The reaction rate distributions of various activation detectors on the cylindrical surface of a tungsten target bombarded with 0.8 and 1.2 GeV protons were analyzed with the NMTC/JAERI-MCNP-4A code system. It was found through the comparison with the experimental results that the code system predicted the reaction rates induced by the sub-10 MeV neutrons with an accuracy of 10 to 15%. Considering that some approximations are included in both the nuclear reaction and particle transport calculation parts of NMTC/JAERI, the accuracy of the code is reasonable.

For the activation detectors sensitive to the neutrons with tens of MeV, however, the agreement between the calculated and experimental results reduced and the C/E ratio was in the level of 50 to 75%. These results suggested that NMTC/JAERI estimated the neutrons in tens of MeV region too low. This feature of NMTC/JAERI was consistent with the conclusion obtained from the other work on neutron spectra measurement and should be improved by further studies from both the microscopic and macroscopic point of view.

References

[1] Venneri F., Bowman C. D., Wender S. A.: "The Physics Design of Accelerator-Driven Transmutation Systems", Proc. of Int. Conf. on Evaluation of Emerging Nuclear Fuel Cycle Systems, GLOBAL '95,

Sep. 11-14, 1995, Versailles, France, pp. 474-481 (1995).
[2] Takizuka T., Nishida T., Sasa T., Takada H., Meigo S., Mizumoto M., Hasegawa K.: Research and Development on Proton Accelerator Based Trans,mutation of Nuclear Waste", *ibid.*, pp. 489-496.
[3] Takahashi, H., Rief, H.: "Concept of Accelerator Based Transmutation Systems", Proc. of the Specialists' Mtg. on Accelerator-Based Transmutation, PSI, Villigen, Switzerland, Mar. 24-26, 1992, pp. 2-26 (1992).
[4] Chuvilo I. V., Kiselev G. V., Bergelson B. R., Kochurov B. P.: "Nuclear Fuel Cycle Using Nuclear Power Facilities Based on Subcritical Blankets Driven by the Proton Accelerator", Proc. of Int. Conf. and Technol. Exposition on Future Nucl. Systems: Emerging Fuel Cycles and Waste Disposal Options, GLOBAL '93, Sep. 12-17, 1993, Seattle, Washington, pp. 924-933 (1995).
[5] Rubbia C., Rubio J. A., Buono S., Carminati F., Fiétier N., Galvez J., Gelès C., Kadi Y., Klapisch R., Mandrillon P., Revol J. P., Roche Ch.:"Conceptual Design of A Fast Neutron operated high Power Energy Amplifier", CERN/AT/95-44 (ET), (1995).
[6] Prael R. E., Lichtenstein H.: LA-UR-89-3014, "Users Guide to LCS: The LAHET Code System", (1989).
[7] Cloth P., Filges D., Neef R. D., Sterzenbach G., Reul Ch., Armstrong T. W., Colborn B. L., Anders B., Brückmann H.: "HERMES A Monte Carlo Program System for Beam Materials Interaction Studies", Jül-2203, (1988).
[8] Nakahara Y., Tsutsui T.: "NMTC/JAERI A Code System for High Energy Nuclear Reactions and Nucleon-Meson Transport Code", JAERI-M 82-198, (1982), [in Japanese].
[9] Emmett M. B.: "The MORSE Monte Carlo Radiation Transport Code System", ORNL-4972, (1975).
[10] Briesmeister J.F. (Ed.) : MCNP A General Monte Carlo N-Particle Transport Code, Version 4A, LA-12625, (1993).
[11] OECD/NEA: "Proc. of Specialists' Mtg. on Intermediate Energy Nucl. Data: Models and Codes", May 31 - June 1, Issy-les-Moulineaux, OECD Publications, Paris, (1994).
[12] Filges D., Nagel P., Neef R. D. (Eds.): "International Code Comparison for Intermediate Energy Nucl. Data: The Thick Target Benchmark", NEA/NSC/DOC(95)-2, (1995).;Sobolevsky N. : "Conclusions of International Code Comparison for Intermediate Energy Nucl. Data, Thick Target Benchmark for Lead and Tungsten", NEA/NSC/DOC(96)-15, (1996).
[13] Michel R., Nagel P.:"Specifications for An International Codes and Model Intercomparison for Intermediate Energy Activation Yields", NEA/NSC/DOC(95)-8, (1995).
[14] Takada H., Hasegawa K., Sasa T., Meigo S., Kanno I.: "Integral Spallation Experiment with a Thick Lead Assembly Irradiated with 500 MeV Protons", Proc. of the 1992 Symp. on Nucl. Data, Nov. 26-27, JAERI, Tokai, Japan, JAERI-M 93-046, pp. 72-81 (1993).
[15] Nakamoto T., Ishibashi K., Matsufuji N., Maehata K., Shigyo N., Meigo S., Takada H., Chiba S., Numajiri M., Wakuta, Y., Watanabe Y.: J. Nucl. Sci. Technol., 32, 827 (1995).
[16] Meigo S. Takada H., Chiba S., Nakamoto T., Ishibashi K., Matsufuji N., Maehata K., Shigyo N., Wakuta, Y., Watanabe Y., Numajiri M.: "Measurements of Spallation Neutrons from a Thick Lead Target Bombarded with 0.5 and 1.5 GeV Protons", Joint Proc. of the 13th Mtg. of the Int. Collaboration on Advanced Neutron Sources held at Paul Scherrer Institute, Oct. 11-14, 1995 and 4th Plenary Mtg. of the European Spallation Source Project, ESS, held at Weinfelden, Oct. 16-19, 1995, PSI-Proceedings 95-02, pp. 442-453 (1995).
[17] Nakao N., Nakashima H., Nakamura T., Tanaka Sh., Tanaka Su., Shin K., Baba M., Sakamoto Y., Nakane Y.: Nucl. Sci. Eng. 124, (1996), (to be published).
[18] Nakashima H., Nakao N., Nakamura T., Tanaka Sh., Shin K., Tanaka Su., Takada H., Meigo S., Nakane Y., Sakamoto Y., Baba M.: *ibid.*, (to be published).
[19] Bertini H. W.: Phys. Rev., 188, 1711 (1969).
[20] Dresner L. W.: ORNL-TM-196, "EVAP - A Fortran Program for Calculating the Evaporation of Various Particles from Excited Compound Nuclei", (1962).
[21] Nakahara Y.: J. Nucl. Sci. Technol., 20, 511 (1983).
[22] Niita K., Chiba S., Maruyama T., Takada, H., Fukahori T., Nakahara, Y., Iwamoto A.: Phys. Rev. C 52, 2620 (1995).[23] Cugnon, J., Mizutani, T., Vandenmuren, J.: Nucl. Phys. A352, 505 (1981); Cugnon, J.: Phys. Rev. C 22, 1885 (1980).
[24] Ignatyuk A. V., Smirenkin G. N., Tishin A. S.: Sov. J. Nucl. Phys., 21, 256 (1975).

[25] Mengoni A., Nakajima Y.: J. Nucl. Sci. Technol., 31, 151 (1994).
[26] Pearlstein, S.: Astrophys. J., 346, 1049 (1989).
[27] Kosako, K., Maekawa, F., Oyama, Y., Uno, Y., Maekawa, H.:"FSXLIB-J3R2 : A Continuous Energy Cross Section Library for MCNP Based on JENDL-3.2", JAERI-Data/Code 94-020, (1994).
[28] Shibata K., Nakagawa T., Asami T., Fukahori T., Narita T., Chiba S., Mizumoto M., Hasegawa A., Kikuchi Y., Nakajima Y., Igarasi S. : "Japanese Evaluated Nuclear Data Library, Version-3 -JENDL-3-", JAERI-1319, (1990); Nakagawa T., Shibata K., Chiba S., Fukahori T., Nakajima Y., Kikuchi Y., Kawano T., Kanda Y., Ohsawa T., Matsunobu H., Kawai M., Zukeran A., Watanabe T., Igarasi S., Kosako K., Asami T.: J. Nucl. Sci. Technol., 32, 1259 (1995).
[29] Kotegawa H., Nakane Y., Hasegawa A., Tanaka Sh.:"Neutron-photon Multigroup Cross Sections for Neutron Energies up to 400 MeV; HILO86R", JAERI-M 93-020, (1993).
[30] Nakazawa M., Kobayashi K., Iwasaki S., Iguchi T., Sakurai K., Ikeda Y., Nakagawa T.: "JENDL Dosimetry File", JAERI-1325, (1992).
[31] Fukahori T.:"ALICE-F Calculation of Nuclear Data up to 1 GeV", Proc. of the Specialists' Mtg. on High Energy Nucl. Data, Oct. 3-4, 1991, JAERI, Tokai, JAERI-M 92-039, pp. 114-122 (1992).
[32] Kim E., Nakamura T., Konno A., Imamura M., Nakao N., Shibata T., Uwamino Y., Nakanishi N., Tanaka Su., Nakashima H., Tanaka Sh.: "Measurement of Neutron Spallation Cross Sections", Proc. of the 1995 Symp. on Nucl. Data, Nov. 16-17, 1995, JAERI, Tokai, Japan, JAERI-Conf 96-008, pp. 236-241 (1996), and private communication.

Table 1. Physical characteristics of activation detectors.

Sample	Size (mm)	Density (g/cc)	Purity (%)
P	20ϕ x 3	2.20	100
S	20ϕ x 3	2.07	95.02
Al	25 x25x1.6	2.699	100
Bi	20ϕ x 1	9.747	99.99

Table. 2. Nuclear characteristics of activation detectors.

Reaction	Half-Life	γ-/β-ray Energy	Emission Rate	Threshold Energy
$^{32}S(n,p)^{32}P$	14.3 days	694.7 keV (β)	1.0	0.96 MeV
$^{31}P(n,p)^{31}Si$	157.3 min	595.7 keV (β)	0.999	0.73 MeV
$^{27}Al(n,p)^{27}Mg$	9.45 min	843 keV (γ)	0.7	1.9 MeV
$^{27}Al(n,\alpha)^{24}Na$	15.0 hours	1369 keV (γ)	1.0	3.27 MeV
$^{209}Bi(n,4n)^{206}Bi$	6.243 days	803.1 keV (γ)	0.989	22.56 MeV
$^{209}Bi(n,5n)^{205}Bi$	15.31 days	703.4 keV (γ)	0.311	29.63 MeV
$^{209}Bi(n,6n)^{204}Bi$	11.22 hours	374.7 keV (γ)	0.737	37.99 MeV
$^{209}Bi(n,7n)^{203}Bi$	11.76 hours	820.2 keV (γ)	0.296	45.31 MeV

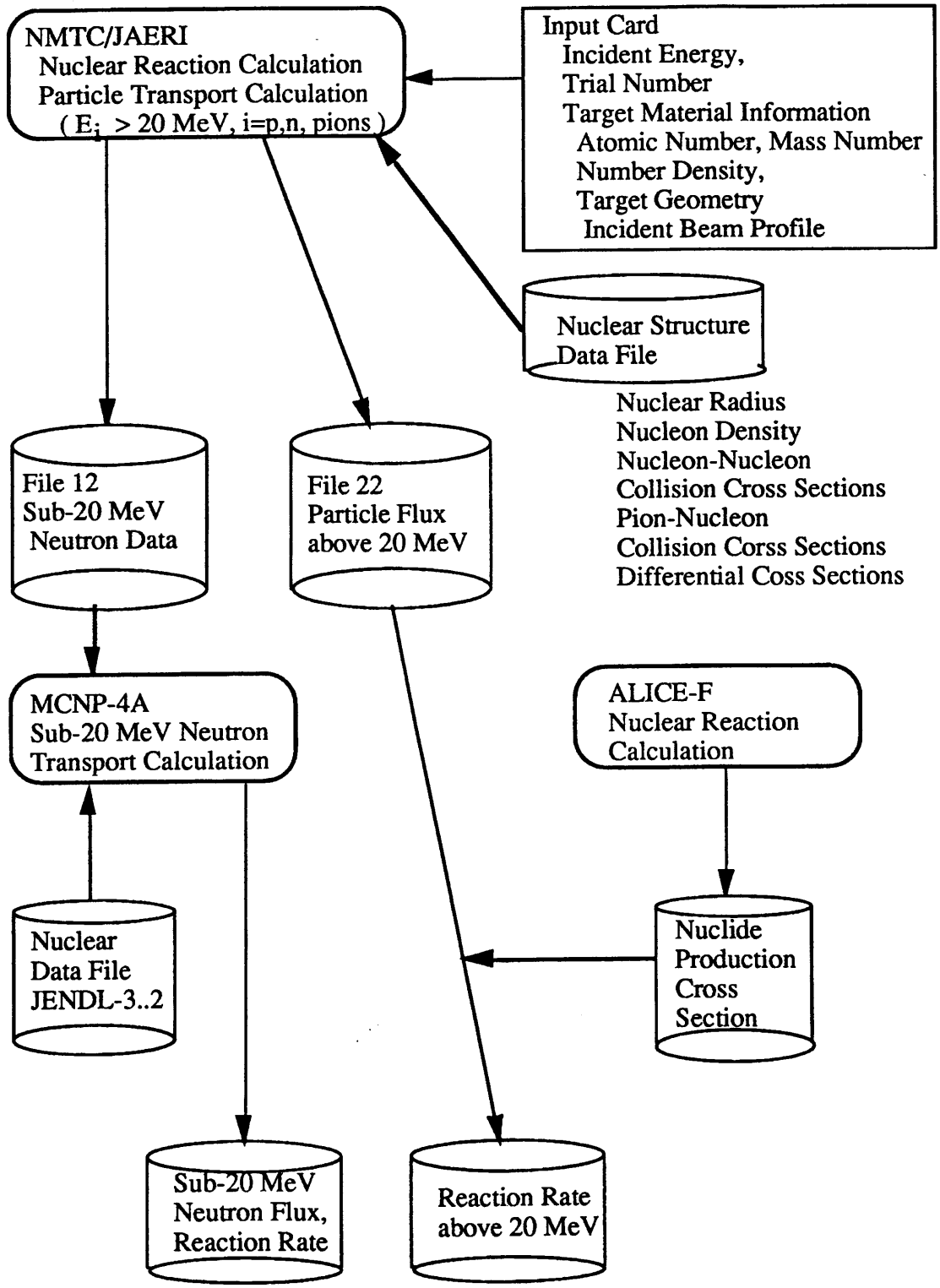

Fig. 1. Calculation flow of the NMTC/JAERI-MCNP-4A code system.

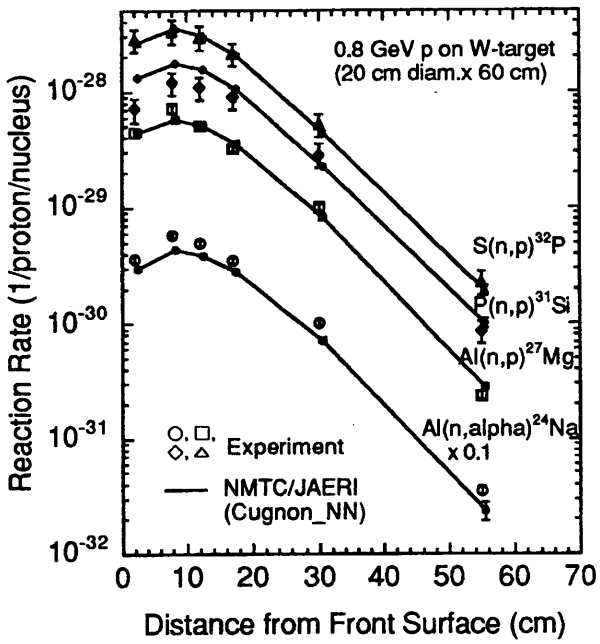

Fig. 2 Experimental and calculated reaction rates of $S(n,p)^{32}P$, $P(n,p)^{31}Si$, $Al(n,p)^{27}Mg$ and $Al(n,\alpha)^{24}Na$ for the 0.8 GeV proton incidence on the thick tungsten target. The open and solid marks indicate the experimental and calculated results of NMTC/JAERI-MCNP-4A, respectively. The lines are for eye-guide.

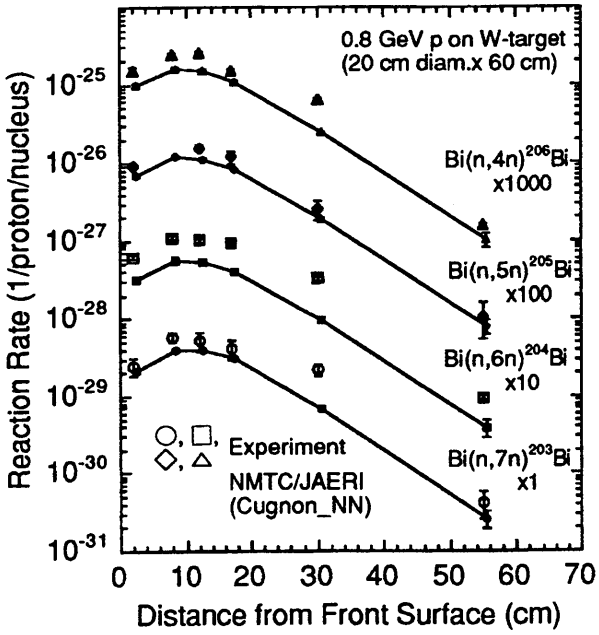

Fig. 3. Experimental and calculated reaction rates of $Bi(n,4n)^{206}Bi$, $Bi(n,5n)^{205}Bi$, $Bi(n,6n)^{204}Bi$ and $Bi(n,6n)^{203}Bi$ for the 0.8 GeV proton incidence on the thick tungsten target. The notes to the marks and lines are the same as for Fig. 2.

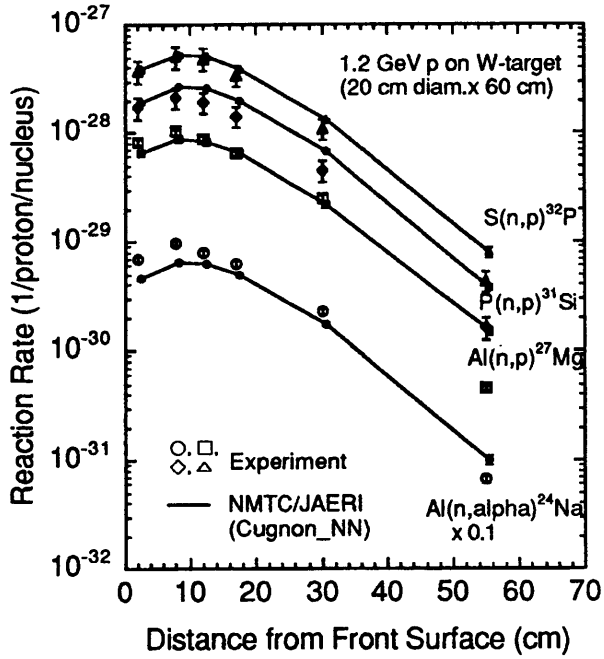

Fig. 4. Experimental and calculated reaction rates of $S(n,p)^{32}P$, $P(n,p)^{31}Si$, $Al(n,p)^{27}Mg$ and $Al(n,\alpha)^{24}Na$ for the 1.2 GeV proton incidence on the thick tungsten target. The notes to the marks and lines are the same as for Fig. 2.

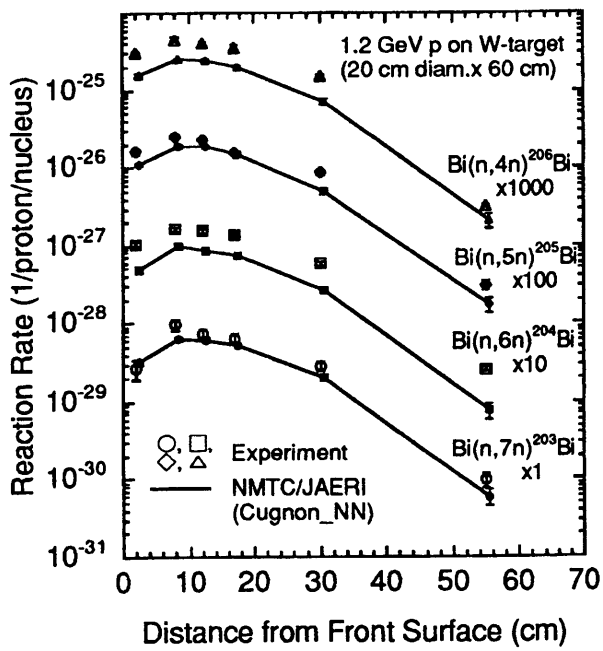

Fig. 5. Experimental and calculated reaction rates of $Bi(n,4n)^{206}Bi$, $Bi(n,5n)^{205}Bi$, $Bi(n,6n)^{204}Bi$ and $Bi(n,6n)^{203}Bi$ for the 1.2 GeV proton incidence on the thick tungsten target. The notes to the marks and lines are the same as for Fig. 2.

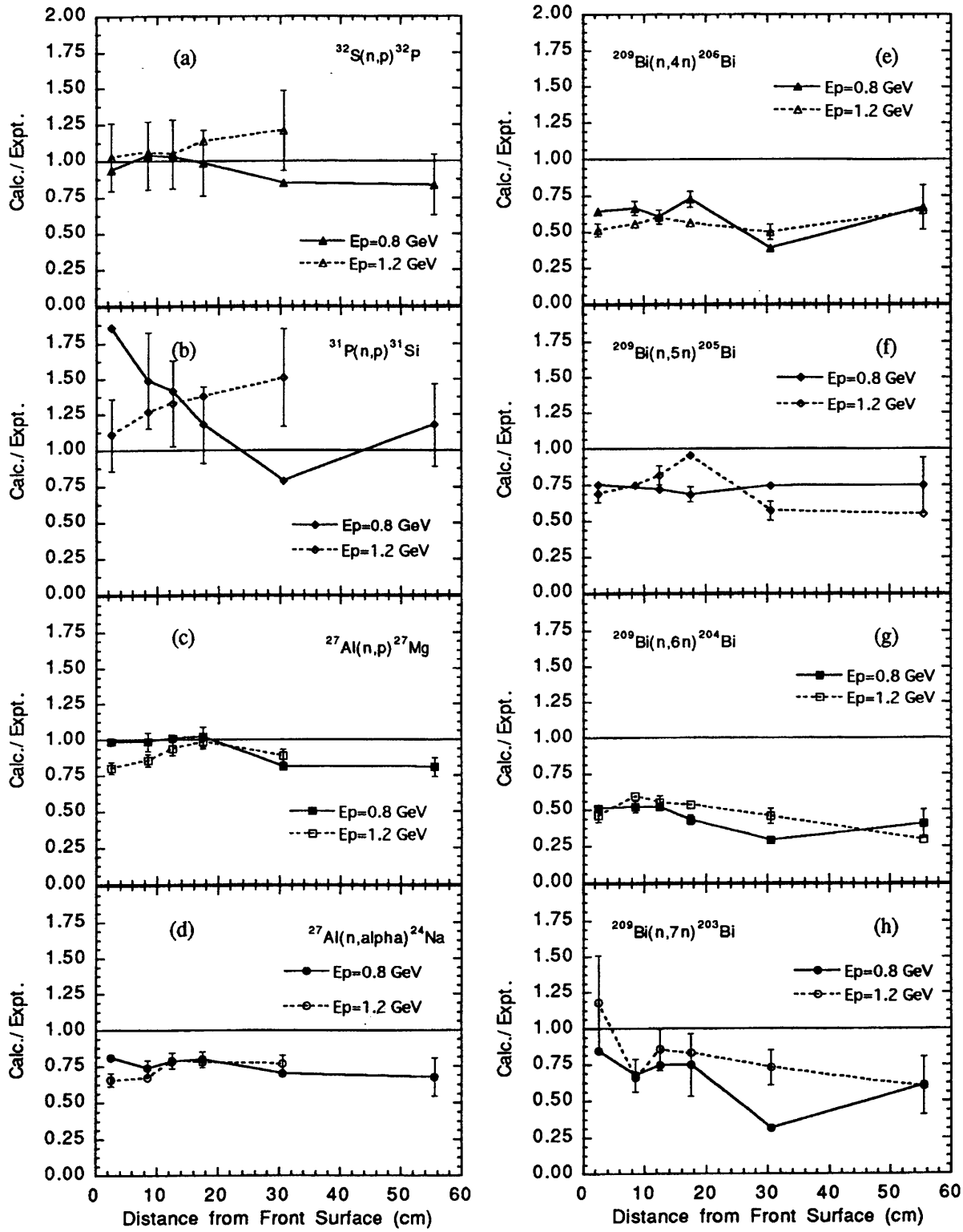

Fig. 6. C/E ratios between the calculated and experimental reaction rates of the activation detectors : (a) $^{32}S(n, p)^{32}P$ reaction, (b) $^{31}P(n, p)^{31}Si$ reaction, (c) $^{27}Al(n, p)^{27}Mg$ reaction, (d) $^{27}Al(n, \alpha)^{24}Na$ reaction, (e) $^{209}Bi(n, 4n)^{206}Bi$ reaction, (f) $^{209}Bi(n, 5n)^{205}Bi$ reaction, (g) $^{209}Bi(n, 6n)^{204}Bi$ reaction, (h) $^{209}Bi(n, 7n)^{203}Bi$ reaction. The solid and open marks indicate the results of the 0.8 and 1.2 GeV proton incidence, respectively. The lines are for eyeguide.

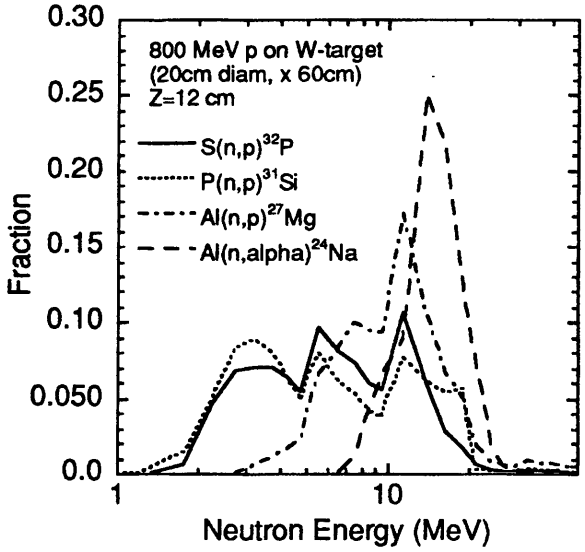

Fig. 7. Sensitivity of the reaction rates to the neutron energy for $S(n,p)^{32}P$, $P(n,p)^{31}Si$, $Al(n,p)^{27}Mg$ and $Al(n,\alpha)^{24}Na$ at the distance of 12cm from front surface.

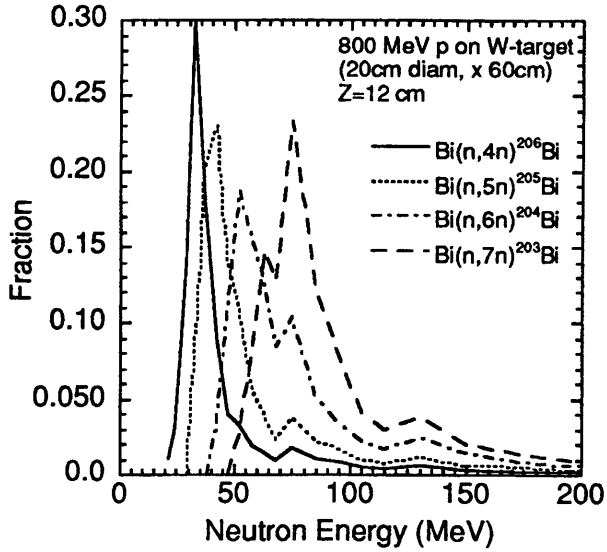

Fig. 8. Sensitivity of the reaction rates to the neutron energy for $Bi(n,4n)^{206}Bi$, $Bi(n,5n)^{205}Bi$, $Bi(n,6n)^{204}Bi$ and $Bi(n,7n)^{203}Bi$ at the distance of 12cm from front surface.

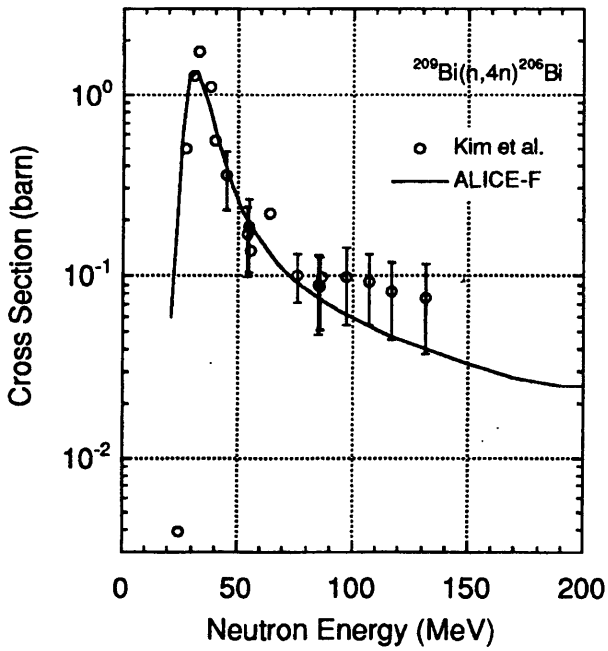

Fig. 9. Experimental and calculated cross section of $^{209}Bi(n,4n)^{204}Bi$. The open marks indicate the experimental data[32]. The solid lined represents the calculated results of ALICE-F.

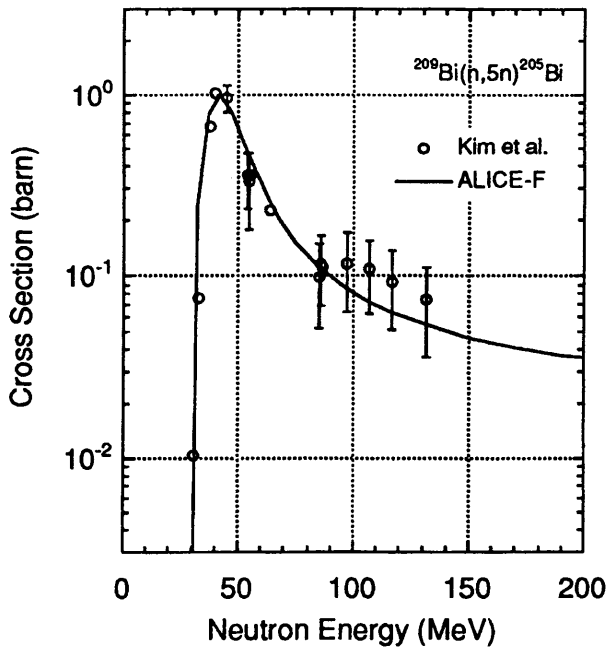

Fig. 10. Experimental and calculated cross section of $^{209}Bi(n,5n)^{205}Bi$. The notes to the marks and lines are the same as for Fig. 9.

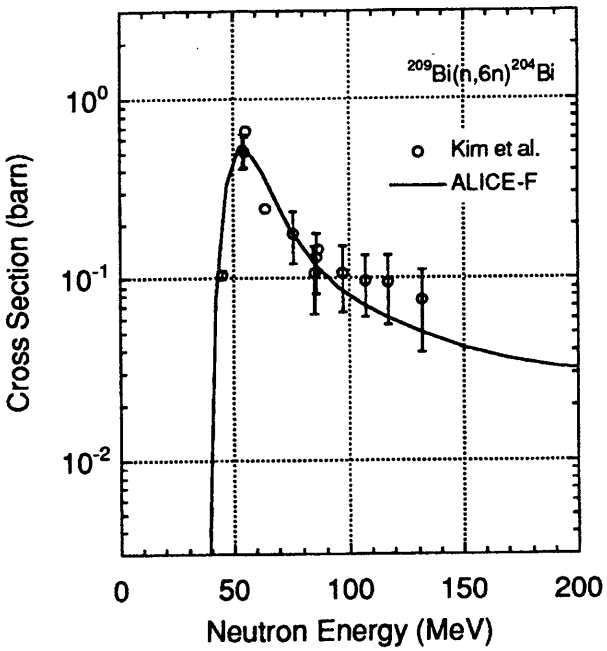

Fig. 11. Experimental and calculated cross section of ^{209}Bi(n,6n)^{204}Bi. The notes to the marks and lines are the same as for Fig. 9.

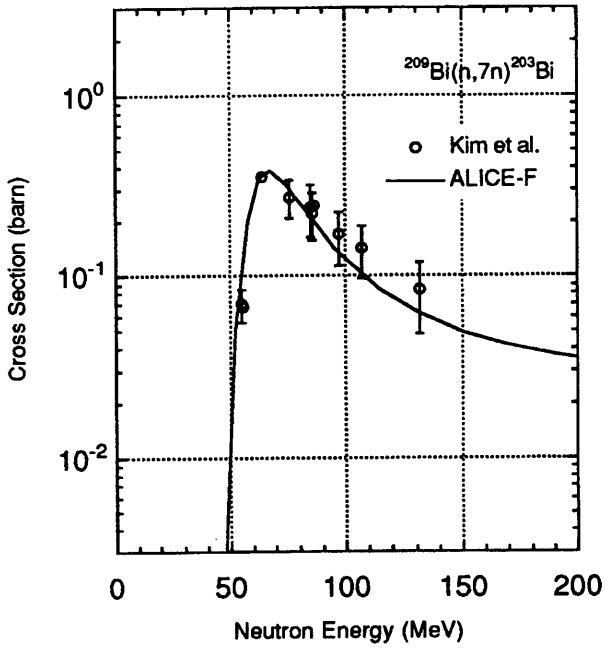

Fig. 12. Experimental and calculated cross section of ^{209}Bi(n,7n)^{203}Bi. The notes to the marks and lines are the same as for Fig. 9.